$5f^3 \rightarrow 5f^26d^1$ Absorption Spectrum Analysis of U^{3+}−$SrCl_2$

Mirosław Karbowiak*

Faculty of Chemistry, University of Wrocław, ul. F. Joliot-Curie 14, 50-383 Wrocław, Poland

Received: November 21, 2004; In Final Form: February 23, 2005

The $5f^3 \rightarrow 5f^26d^1$ absorption spectra of the U^{3+} ions incorporated in $SrCl_2$ single crystals were recorded at 4.2 K in the 15 000−50 000 cm^{-1} spectral range. From an analysis of the vibronic structure, 32 zero-phonon lines corresponding to transitions from the $^4I_{9/2}$ ground multiplet of the $5f^3$ configuration to the $5f^26d(e_g)^1$ excited levels were assigned. A theoretical model proposed by Reid et al. (Reid, H. F.; van Pieterson, L.; Wegh, R. T.; Meijerink, A. *Phys. Rev. B* **2000**, *62*, 14744) that extends the established model for energy-level calculations of nf^N states has been applied for analysis of the spectrum. The $F^k(ff)$ ($k = 2, 4$), $\zeta_{5f}(ff)$, $B^4_0(ff)$, $B^6_0(ff)$, $F^k(fd)$ ($k = 2, 4$), and $G^j(fd)$ ($j = 1, 3$) Hamiltonian parameters were determined by a least-squares fitting of the calculated energies to the experimental data. A good overall agreement between the calculated and experimentally observed energy levels has been achieved, with the root-mean-square (rms) deviation equal to 95 cm^{-1} for 32 fitted levels and 9 varied parameters. Adjusted values of $F^k(ff)$ and $\zeta_{5f}(ff)$ parameters for the $5f^2$ core electrons are closer to the values characteristic of the $5f^2$ (U^{4+}) configuration than to those of the $5f^3$ (U^{3+}) configuration. For the U^{3+} ion, the *f*−*d* Coulomb interaction parameters are significantly more reduced from the values calculated using Cowan's computer code than they are for lanthanide ions. Moreover, because of weaker *f*−*d* Coulomb interactions for the U^{3+} ion than for the isoelectronic Nd^{3+} lanthanide ion, the very simple model assuming the coupling of crystal-field levels of the $6d^1$ electron with the lattice and the multiplet structure of the $5f^2$ configuration may be employed for the qualitative description of the general structure of the U^{3+} ion *f*−*d* spectrum.

1. Introduction

The first strong absorption bands due to the parity-allowed f−d transition of U^{3+} ions incorporated into chloride lattices appear as low as ~15 000 cm^{-1} above the ground $^4I_{9/2}$ state,[1] which makes the $5f^3 \rightarrow 5f^26d^1$ transitions more accessible experimentally as compared, for example, with Ln^{3+} ions, for which the $4f^N \rightarrow 4f^{N-1}5d^1$ absorption bands are observed in the UV and VUV regions at much higher energies.[2]

The first attempts of an analysis of uranium(3+) $5f^3 \rightarrow 5f^2$-$6d^1$ transitions have been reported for solution spectra by Kaminskaya et al.[3,4] and for the solid state by Mazurak et al.[5] An interpretation of the $5f^3 \rightarrow 5f^26d^1$ bands observed in the room-temperature absorption spectrum of U^{3+}-doped Cs_2NaYCl_6 single crystals has been presented in ref 6. The interpretation was based on the assumption that the $5f^26d^1$ configuration behaves according to the $J_1\gamma_n$ coupling scheme, where J_1 is the total angular momentum of a Russell−Saunders term derived for the $5f^2$ core, and $J_1\gamma_n$ is a state of the 6d electron in the crystal field. A comprehensive survey of the $5f^N \rightarrow 5f^{N-1}6d^1$ absorption spectra of U^{4+}- and U^{3+}-doped Cs_2NaYCl_6, Cs_2LiYCl_6, Cs_2NaYBr_6, $CsCdBr_3$, and $Cs_3Lu_2Cl_9$ single crystals has been reported in ref 1. Recently, a paper reporting ab initio theoretical studies of the structure and spectroscopy of U^{3+} in Cs_2NaYCl_6 single crystals has appeared.[7]

The number of papers dealing with the f−d transitions of lanthanide ions is significantly larger than that for actinide ions. However, in most cases, the structure of the observed $4f^N \rightarrow 4f^{N-1}5d^1$ transitions has been rationalized in the simple one-electron model[8,9] or with the assumption that the excited configurations were formed by a coupling of the split by the crystal-field 5d orbitals with the $4f^{N-1}$ core electrons and lattice vibrations.[10−13] Recently, $4f^N \rightarrow 4f^{N-1}5d^1$ transitions of Ln^{3+} ions incorporated in $LiYF_4$, CaF_2, and YPO_4 host lattices have been recorded in the UV and VUV spectral region (100−250 nm) and were analyzed. A theoretical model for the calculation of the $4f^{N-1}5d^1$ energy levels has been applied, which extends the established model for the $4f^N$ configuration by including crystal-field and spin−orbit interactions for the 5d electron as well as the Coulomb interactions between the 4f and 5d electrons.[14−16] The same procedure has been applied recently for modeling of the $5f^3 \rightarrow 5f^26d^1$ absorption spectrum of U^{3+} in $LiYF_4$.[17] However, in view of the limited number of available experimental energies of the $nf^{N-1}(n+1)d^1$ configuration, the Hamiltonian parameters could not have been obtained from the fit to the experimental energies, as is usually done for nf^N configuration. In the applied approach, parameters describing the interactions of the nf^{N-1} core electrons were approximated by the literature values for the nf^N configuration. The parameters for Coulomb *f*−*d* interactions as well as for the spin−orbit interaction of the $(n+1)d^1$ electron were calculated ab initio and then adjusted to values providing the best agreement between the calculated and experimental spectra.

In this paper, we present the results of the application of the above-mentioned model for the calculation of the $5f^26d^1$ energy levels of U^{3+} in $SrCl_2$ single crystals. During a crystal growth, Na^+ was used as a charge compensator to favor the formation of O_h sites for U^{3+} ions. The vibronic structure observed for the $5f^3 \rightarrow 5f^26d^1$ absorption spectra recorded at 4.2 K in the 15 000−50 000 cm^{-1} spectral range was analyzed. The relatively large number of experimentally determined energies of crystal-field components enabled the adjustment of the values of the $F^k(ff)$ ($k = 2, 4$), $\zeta_{5f}(ff)$, $B_0^4(ff)$, $B_0^6(ff)$, $F^k(fd)$ ($k = 2, 4$), and $G^j(fd)$ ($j = 1, 3$) Hamiltonian parameters in the least-squares

* Corresponding author. E-mail: karb@wchuwr.chem.uni.wroc.pl. Tel: +48 71 3757304. Fax: +48 3282348.

10.1021/jp044690v CCC: $30.25
Published on Web 03/26/2005

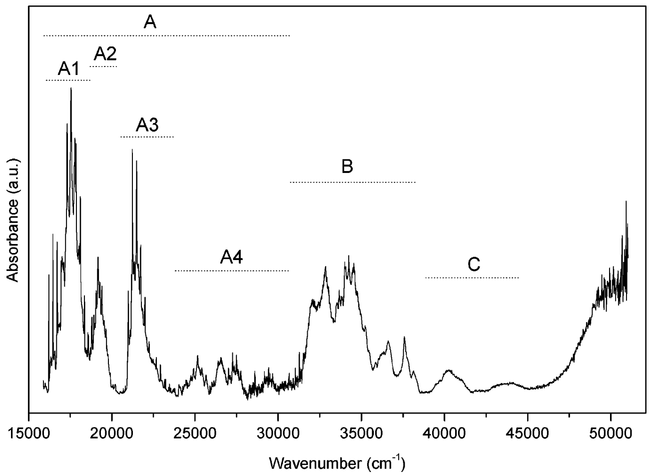

Figure 1. Survey of the $5f^3 \rightarrow 5f^2 6d^1$ absorption spectrum at 7 K of $U^{3+}-SrCl_2$.

procedure. The obtained values are discussed and compared to those that were determined for lanthanide ions.

2. Experimental Section

Uranium(3+)-doped single crystals of $SrCl_2$ with a nominal 0.05 mol % uranium concentration were grown by the Bridgman−Stockbarger method. NaCl was added as a charge compensator. Dry $SrCl_2$ powder was mixed with an appropriate amount of NaCl and UCl_3, placed in a vitreous carbon crucible, and sealed under argon in silica ampules. UCl_3 has been obtained by the thermal decomposition of $NH_4UCl_4 \cdot 4H_2O$ according to the procedure reported in ref 18. The doped single crystals were cut and polished under dry paraffin oil. The absorption spectra were recorded on a Cary-50 UV−Vis NIR spectrophotometer in the 15 000−50 000 cm^{-1} range. An Oxford Instrument model CF1204 cryostat was used for low-temperature measurements.

3. Results

In a 7 K survey absorption spectrum of $U^{3+}-SrCl_2$, which is presented in Figure 1, three groups of bands, arbitrarily labeled A, B, and C, could be distinguished. Groups A and B consist of strong bands with a fine structure. However, although for group A one may easily identify the a_{1g} vibronic progressions, no such vibronic pattern may be distinguished in group B. The bands forming group C are less intense and do not possess a fine structure.

Comparison of the $U^{3+}-SrCl_2$ spectrum with those reported for U^{3+} in other host crystals[1] enables the assignment of the lines observed in the 16 000−32 000 cm^{-1} range (Figure 1, group A) as transitions from the $^4I_{9/2}(5f^3)$ ground multiplet to the $5f^2 6d(e_g)^1$ crystal field levels of U^{3+} ions. The broad bands without fine structure, observed in the 38 000−46 000 cm^{-1} range (Figure 2, group C) should be assigned as transitions to the $5f^2 6d(t_{2g})^1$ crystal field levels of U^{3+}. The bands between 32 000 and 38 000 cm^{-1} may be attributed tentatively to f−d transitions of U^{4+} ions present as impurities in the crystal under investigation.

Figure 2 shows the absorption spectrum of $U^{3+}-SrCl_2$ in detail in the lowest energy part of the $^4I_{9/2} \rightarrow 5f^2 6d(e_g)^1$ transition range (groups A1 and A2 in Figure 1). The most prominent feature of the spectrum is the ~247-cm^{-1} vibronic progression that arises from the totally symmetric $\nu_1(a_{1g})$ stretch of the UCl_8^{3-} moiety. The lowest-energy zero-phonon line is distinctly observable at 16 213 cm^{-1} (line 1). For this line, the $\nu_1(a_{1g})$ progression extends through at least three quanta. The next two zero-phonon lines could be localized readily at 17 310 and 17 606 cm^{-1}, and for both of them, progressions up to the third one, based on the a_{1g} mode, are easily perceptible. The careful analysis of the spectrum enabled the assignment of zero-phonon lines at 16 330, 16 736, 16 869, and 17 007 cm^{-1} also. The band in the 18 500−20 000 cm^{-1} spectral region is composed of vibronic satellites accompanying the zero-phonon lines at 18 563, 18 599, 18 727, and 18 918 cm^{-1}. In Figure 2, the determined positions of the zero-phonon transitions are marked with arrows, whereas the $\nu_1(a_{1g})$ vibronic progressions coupled to each of the zero-phonon line are indicated by dotted vertical lines.

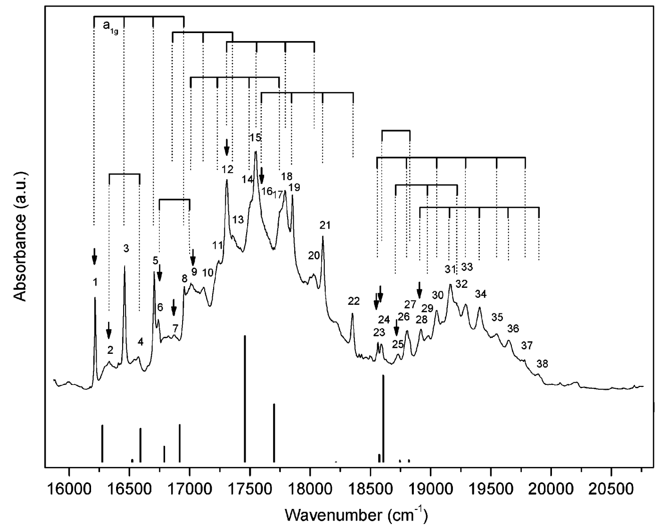

Figure 2. Absorption spectrum recorded at 7 K for the $U^{3+}-SrCl_2$ single crystal in the $5f^3(^4I_{9/2}) \rightarrow 5f^2 6d(e_g)^1$ transition range. The zero-phonon lines are marked with arrows, whereas the vibronic progressions are indicated by dotted lines. The numbering of the lines corresponds to that in column 1 of Table 1. The sticks at the bottom of the figure indicate the calculated positions of the zero-phonon lines, with the heights proportional to the predicted intensities.

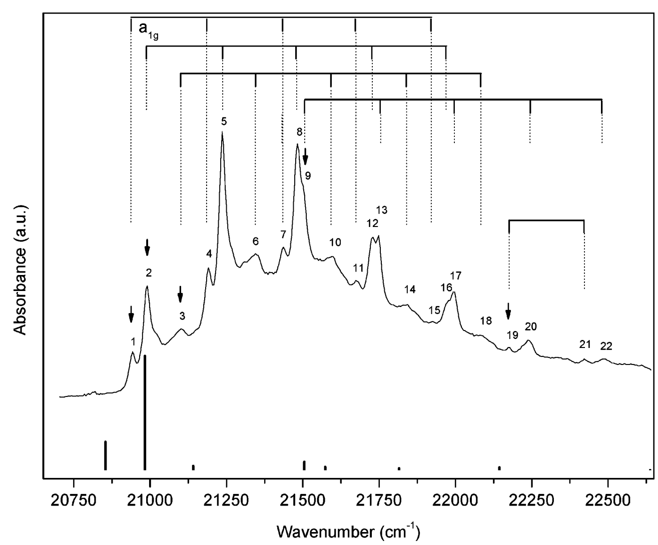

Figure 3. Absorption spectrum recorded at 7 K for the $U^{3+}-SrCl_2$ single crystal in the $5f^3(^4I_{9/2}) \rightarrow 5f^2 6d(e_g)^1$ transition range. The zero-phonon lines are marked with arrows, whereas the vibronic progressions are indicated by dotted lines. The numbering of the lines corresponds to that in column 4 of Table 1. The sticks at the bottom indicate the calculated positions of the zero-phonon lines, with the heights proportional to the predicted intensities.

Figure 3 shows a high-resolution absorption spectrum recorded for $U^{3+}-SrCl_2$ in the 20 750−22 750 cm^{-1} spectral

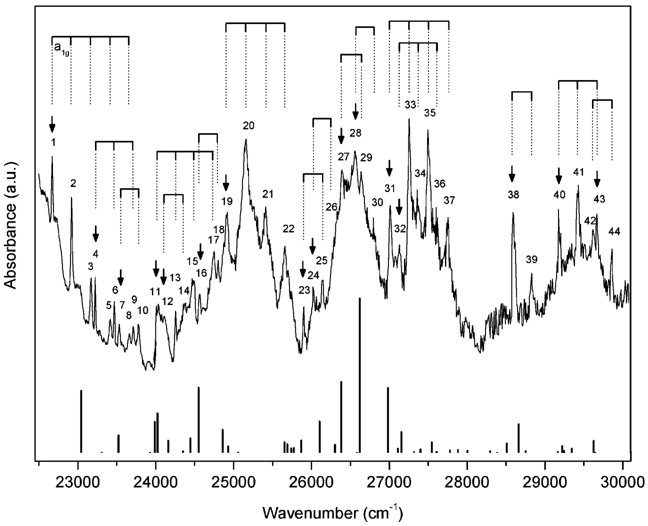

Figure 4. Absorption spectrum recorded at 7 K for the $U^{3+}-SrCl_2$ single crystal in the $5f^3(^4I_{9/2}) \rightarrow 5f^26d(e_g)^1$ transition range. The zero-phonon lines are marked with arrows, whereas the vibronic progressions are indicated by dotted lines. The numbering of the lines corresponds to that in column 7 of Table 1. The sticks at the bottom of the figure indicate the calculated positions of the zero-phonon lines, with the heights proportional to the predicted intensities.

region. The observed absorption band is built up from the ν_1-(a_{1g}) vibronic progressions, extending through at least four quanta, coupled to the zero-phonon lines at 20 942, 20 991, 21 101, and 21 502. The lower-intensity zero-phonon line was also determined at 22 178 cm^{-1}.

In the region above 22 500 cm^{-1} presented in Figure 4, the vibronic pattern is not as clearly resolved as it was for lower energy bands. Nevertheless, the positions of 16 zero-phonon lines could have been determined.

The energies of the zero-phonon lines and the vibronic satellites identified in the $5f^3 \rightarrow 5f^26d(e_g)^1$ transition range of the U^{3+} ion in $SrCl_2$ that are associated with them are given in Table 1.

4. Discussion

4.1. $5f^3 \rightarrow 5f^26d^1$ Transitions. Strontium chloride crystallizes in a fluorite-type structure and is isostructural with CaF_2. In these types of host crystals, trivalent ions substitute for the divalent metal ion mostly at sites of C_{4v} and C_{3v} symmetry, with the charge compensation provided by the interstitial fluoride ion. However, in the presence of monovalent impurity ions (e.g., Na^+), formation of O_h sites is privileged.[19] Therefore, one may assume that in $SrCl_2$ doped with UCl_3 and NaCl the U^{3+} ions possess O_h-site symmetry. This assumption is supported by the lack of U^{3+} f → f transitions (forbidden for O_h) in regions below 16 000 cm^{-1} for crystals codoped with NaCl, whereas such lines are observable for crystals grown in the absence of NaCl.

In contrast to U^{3+}-doped elpasolite crystals, in which different vibronic electric dipole transitions ($\nu_2(e_g)$ and $\nu_5(t_{2g})$ as well as lattice modes) are superimposed on the a_{1g} progression forming a rather complex vibronic structure,[1] in the f−d spectrum of $U^{3+}-SrCl_2$, the observed phonon lines correspond to the ∼247 cm^{-1} $\nu_1(a_{1g})$ symmetric stretching mode exclusively. The Huang−Rhys parameter (S) may be evaluated from the following equation

$$I_n \propto e^{-S}\left(\frac{S^n}{n!}\right) \qquad (1)$$

where I_n is the intensity and n is the vibrational quantum number of the terminal state.[20] However, because vibronic progressions coupled to different ZP lines overlap in the analyzed spectral region, the accurate determination of vibronic intensities was not possible. By taking into account the integrated area of vibronic peaks coupled to relatively well separated ZP(1) and ZP(13) lines at 16 213 cm^{-1} (line 1 in Figure 2) and 20 991 cm^{-1} (line 2 in Figure 3), respectively, we obtained the value $S(a_{1g}) \approx 1.5$, which points to a rather weak electron−lattice coupling. Because of a relatively low value of the $S(a_{1g})$ parameter, a significant part of the transition intensity is included in the zero-phonon line, which, in connection with a rather simple vibronic pattern, facilitates interpretation of the spectra. Therefore, almost all of the observed lines could have been assigned, and energies of a large number of zero-phonon transitions have been determined. In the absorption spectrum of $U^{3+}-SrCl_2$, the lowest-energy $5f^3 \rightarrow 5f^26d^1$ transition is observed at 16 213 cm^{-1}, whereas for U^{3+} embedded in Cs_2NaYCl_6 crystals, the first f → d transition appears about 2000 cm^{-1} lower in energy (i.e., at 14158 cm^{-1}). The difference results from shorter Y(U)−Cl distances in the elpasolite crystal, which are equal to 2.619 Å (ref 21), compared to 3.021 Å Sr-(U)−Cl distances in strontium chloride. This leads to a larger covalency of the Cs_2NaYCl_6 lattice and shifts the $5f^26d^1$ configuration toward lower energy (nephelauxetic effect). Moreover, the larger uranium−ligand distances result in smaller crystal-field splitting ($10Dq$) of the $5f^26d^1$ configuration for $U^{3+}-SrCl_2$. The difference in the crystal-field strength is also a consequence of different uranium(3+) coordination geometries in both crystals. The point-charge model predicts that the crystal-field splitting in cubic 8-fold coordination ($SrCl_2$, Δ_o) is intrinsically smaller than that in the octahedral symmetry (Cs_2NaYCl_6 Δ_c), $\Delta_o = -^8/_9\Delta_c$.

The absorption lines observed in the 16 000−32 000 cm^{-1} region (Figure 1, group A) have been assigned as transitions from the lowest level of the $^4I_{9/2}$ ground multiplet of the U^{3+} $5f^3$ configuration to crystal-field levels resulting from the $5f^2$-$6d(e_g)^1$ configuration. At a higher-energy region of the spectrum, one may perceive two groups of bands, labeled B and C in Figure 1. Although the fine structure is discernible for group B, it does not correspond to the vibronic pattern that is characteristic for bands observed at a lower energy (group A). Group C consists of two broad and unstructured bands.

For $CeCl_6^{3-}$, the experimentally determined crystal-field splitting ($10Dq$) amounts to ∼18 500 cm^{-1} (ref 22). Because of the larger spatial extent of 5f and 6d orbitals compared to 4f and 5d orbitals, the crystal-field splitting ($10Dq$) of the $5f^26d^1$ configuration is not expected to be smaller than that observed for the $4f^25d^1$ configuration. This suggests that the lines that formed group C in Figure 1 should be assigned as transitions to the $5f^26d(t_{2g})^1$ configuration of U^{3+} in $SrCl_2$. Such an assignment provides a reasonable $10Dq$ value of ≥20 000 cm^{-1}. Moreover, it is in accordance with the results reported for the $U^{3+}-Cs_2NaYCl_6$ crystal, in which the analogous transitions were observed at an energy higher than 40 700 cm^{-1}, which resulted in a $10Dq$ value of ∼23 000 cm^{-1}.[1]

The energy difference between the barycenters of the bands, labeled in Figure 1 as group B and group A, is smaller than 15 000 cm^{-1}, and consequently, group B cannot be regarded as resulting from transitions to the $5f^26d(t_{2g})^1$ configuration of U^{3+}. However, the theoretical analysis, the details of which are presented in the following sections, excludes the possibility of assignment of these bands as transitions to the $5f^26d(e_g)^1$ configuration. Therefore, one should consider that group B may

TABLE 1: Positions and Assignments of the Zero-Phonon (ZP) and Vibronic Lines Observed in the $5f^3-5f^26d(e_g)^1$ Absorption Transition Range of the U^{3+} Ion in a $SrCl_2$ Single Crystal[b]

group A1 and A2 (16 000−20 000 cm^{-1})			group A3 (20 500−22 500 cm^{-1})			group A4 (22 500−30 000 cm^{-1})		
no.[a]	assignment	line position (cm^{-1})	no.[a]	assignment	line position (cm^{-1})	no.[a]	assignment	line position (cm^{-1})
1	ZP(1)	16 213	1	ZP(12)	20 942	1	ZP(17)	22671
2	ZP(2)	16 330	2	ZP(13)	20 991	2	ZP(17) + ν_1	22671 + 245
3	ZP(1) + ν_1	16 213 + 250	3	ZP(14)	21 101	3	ZP(17) + 2ν_1	22671 + 493
4	ZP(2) + ν_1	16 330 + 241	4	ZP(12) + ν_1	20 942 + 249	4	ZP(18)	23223
5	ZP(1) + 2ν_1	16 213 + 490	5	ZP(13) + ν_1	20 991 + 245	5	ZP(17) + 3ν_1	22671 + 746
6	ZP(3)	16 736	6	ZP(14) + ν_1	21 101 + 246	6	ZP(18) + ν_1	23223 + 247
7	ZP(4)	16 869	7	ZP(12) + 2ν_1	20 942 + 494	7	ZP(19)	23527
8	ZP(1) + 3ν_1	16 213 + 743	8	ZP(13) + 2ν_1	20 991 + 492	8	ZP(17) + 4ν_1	22 671 + 985
9	ZP(5)	17 007	9	ZP(15)	21 502	9	ZP(18) + 2ν_1	23 223 + 488
10	ZP(4) + ν_1	16 869 + 243	10	ZP(14) + 2ν_1	21 101 + 494	10	ZP(19) + ν_1	23 527 + 243
11	ZP(5) + ν_1	17 007 + 237	11	ZP(12) + 3ν_1	20 942 + 736	11	ZP(20)	24 009
12	ZP(6)	17 310	12	ZP(13) + 3ν_1	20 991 + 737	12	ZP(21)	24 123
13	ZP(4) + 2ν_1	16 869 + 495	13	ZP(15) + ν_1	21 502 + 248	13	ZP(20) + ν_1	24 009 + 247
14	ZP(5) + 2ν_1	17 007 + 501	14	ZP(14) + 3ν_1	21 101 + 739	14	ZP(21) + ν_1	24 123 + 243
15	ZP(6) + ν_1	17 310 + 245	15	ZP(12) + 4ν_1	20 942 + 978	15	ZP(20) + 2ν_1	24 009 + 478
16	ZP(7)	17 606	16	ZP(13) + 4ν_1	20 991 + 981	16	ZP(22)	24 564
17	ZP(5) + 3ν_1	17 007 + 748	17	ZP(15) + 2ν_1	21 502 + 492	17	ZP(20) + 3ν_1	24 009 + 739
18	ZP(6) + 2ν_1	17 310 + 487	18	ZP(14) + 4ν_1	21 101 + 981	18	ZP(22) + ν_1	24 564 + 243
19	ZP(7) + ν_1	17 606 + 249	19	ZP(16)	22 178	19	ZP(23)	24 918
20	ZP(6) + 3ν_1	17 310 + 720	20	ZP(15) + 3ν_1	21 502 + 743	20	ZP(23) + ν_1	24 918 + 247
21	ZP(7) + 2ν_1	17 606 + 497	21	ZP(16) + ν_1	22 178 + 243	21	ZP(23) + 2ν_1	24 918 + 489
22	ZP(7) + 3ν_1	17 606 + 744	22	ZP(15) + 4ν_1	21 502 + 985	22	ZP(23) + 3ν_1	24 918 + 740
23	ZP(8)	18 563				23	ZP(24)	25 900
24	ZP(9)	18 599				24	ZP(25)	26 021
25	ZP(10)	18 727				25	ZP(24) + ν_1	25 900 + 244
26	ZP(8) + ν_1	18 563 + 241				26	ZP(25) + ν_1	26 021 + 247
27	ZP(9) + ν_1	18 590 + 241				27	ZP(26)	29 392
28	ZP(11)	18 918				28	ZP(27)	26 560
29	ZP(10) + ν_1	18 727 + 249				29	ZP(26) + ν_1	29 392 + 245
30	ZP(8) + 2ν_1	18 563 + 490				30	ZP(27) + ν_1	26 560 + 243
31	ZP(11) + ν_1	18 918 + 249				31	ZP(28)	27 012
32	ZP(10) + 2ν_1	18 727 + 489				32	ZP(29)	27 130
33	ZP(8) + 3ν_1	18 563 + 725				33	ZP(28) + ν_1	27 012 + 242
34	ZP(11) + 2ν_1	18 918 + 487				34	ZP(29) + ν_1	27 130 + 247
35	ZP(8) + 4ν_1	18 563 + 989				35	ZP(28) + 2ν_1	27 012 + 496
36	ZP(11) + 3ν_1	18 918 + 732				36	ZP(29) + 2ν_1	27 130 + 488
37	ZP(8) + 5ν_1	18 563 + 243				37	ZP(28) + 3ν_1	27 012 + 736
38	ZP(11)+4 ν_1	18 918 + 982				38	ZP(30)	28 590
						39	ZP(30) + ν_1	28 590 + 244
						40	ZP(31)	29 188
						41	ZP(31) + ν_1	29 184 + 241
						42	ZP(32)	29 615
						43	ZP(31) + 2ν_1	29 184 + 486
						44	ZP(32) + ν_1	29 615

[a] Numbers in these columns correspond to the line labels in Figures 2−4. [b] ν_1 is the totally symmetric stretch of the UCl_8^{3-} moiety.

result from f−d transitions of U^{4+} impurities. Unfortunately, it was not possible to prepare the U^{4+}-doped $SrCl_2$ crystals because in the growing conditions, U^{4+} ions underwent a considerable reduction to U^{3+}. Nevertheless, for $SrCl_2$ crystals obtained with UCl_4 instead of UCl_3 as a dopant, one may observe a significant increase of intensity of the band starting at 32 000 cm^{-1} and extending to 38 000 cm^{-1} compared to the bands in the 16 000−32 000 cm^{-1} region, which supports the proposed assignment. Moreover, the positions of the bands of group B correspond well to the energy of the f−d transitions of the U^{4+} ion in the Cs_2NaYCl_6 crystal, for which they have been determined to be between ∼31 000 and 38 000 cm^{-1}.[1]

4.2. Energy-Level Analysis. Recently, Reid[14] proposed that energy levels and intensities of the $nf^N \rightarrow nf^{N-1}(n+1)$d transitions of rare-earth elements can be calculated using a theoretical model for nf^N energy levels extended for interactions related to the presence of the d electron. It is assumed that for the excited $nf^{N-1}(n+1)d^1$ configuration the nf^{N-1} core experiences the same interactions as the nf^N configuration. These interactions are the following: Coulomb interaction between 5f electrons (parametrized by $F^k(ff)$), spin−orbit interaction (parametrized by $\zeta_{nf}(ff)$), two-electron correlation corrections to the Coulomb repulsions (parametrized by $\alpha(ff)$, $\beta(ff)$, and $\gamma(ff)$), three-electron correlations (parametrized by T^i-(ff)), and electrostatically correlated spin−orbit interactions (parametrized by $P^k(ff)$) as well as spin−spin and spin−other orbit interactions (parametrized by $M^j(ff)$). However, because of the presence of the d electron, the atomic part of the Hamiltonian is supplemented by the spin−orbit interactions for the $(n+1)$d electron parametrized by $\zeta(dd)$ and the Coulomb interactions between the $(n+1)$d electron and the nf^{N-1} electrons parametrized by direct $F^k(fd)$ ($k = 2, 4$) and exchange $G^j(fd)$ ($j = 1, 3, 5$) Slater parameters. The crystal-field interactions of the nf^{N-1} and $(n+1)$d electrons with the lattice are parametrized by $B^k_q(ff)$ ($k = 2, 4, 6$) and $B^k_q(dd)$ ($k = 2, 4$), respectively, with the value of q restricted by the site symmetry. The difference in energy between the excited $nf^{N-1}(n+1)$d and ground nf^N configuration is parametrized by $\Delta_E(fd)$. Then, the complete Hamiltonian for the $nf^{N-1}(n+1)$d configuration may be written as[14]

$$\hat{H} = \sum_{k=2,4,6} F^k(ff)\hat{f}_k(ff) + \zeta_{5f}(ff)\hat{A}_{SO}(ff) + \alpha(ff)\hat{L}(\hat{L}+1) + \beta(ff)\hat{G}(G_2) + \gamma(ff)\hat{G}(R_7) + \sum_i T^i(ff)t_i(ff) + \sum_j M^j(ff)\hat{m}_j(ff) + \sum_k P^k(ff)p_k(ff) + \sum_{k,q} B^k_q(ff)C^{(k)}_q(ff) + \Delta_E(fd)\delta_E(fd) + \sum_{k=2,4} F^k(fd)f_k(fd) + \sum_{j=1,3,5} G^j(fd)g_j(fd) + \zeta(dd)A_{SO}(dd) + \sum_{k,q} B^k_q(dd)C^{(k)}_q(dd) \quad (2)$$

This Hamiltonian has been used recently for the modeling of the $4f^N \leftrightarrow 4f^{N-1}5d$ spectra of lanthanide ions doped into $LiYF_4$, YPO_4, and CaF_2 crystals.[15,16] Besides, the $5f^3 \rightarrow 5f^26d$ absorption spectrum of U^{3+} in $LiYF_4$ has been calculated in the frame of this model.[17] In the approach applied in these analyses, the initial values of the Hamiltonian parameters for the nf^{N-1} core were estimated on the basis of the parameters for the nf^N configuration, $(n+1)$d crystal-field parameters were estimated from the analysis of the Ce^{3+} spectrum, and the atomic parameters for the $(n+1)$d electron interactions were estimated from ab initio calculations using Cowan's computer code. Then, the $F^k(fd)$ and $G^j(fd)$ f−d interaction parameters were scaled to obtain the best agreement between the calculated and experimental spectra. In the case of lanthanide ions in fluoride hosts, the best agreement was obtained when the f−d parameters were reduced to about 67% of their free-ion ab initio calculated values,[35] and a much larger reduction to ∼33% of the free-ion value was required for the U^{3+} ion.[17]

Such a procedure was imposed by the fact that the number of assigned zero-phonon lines was small compared to the number of adjustable parameters. In contrast to these studies, analysis of the f−d absorption spectra of U^{3+} in $SrCl_2$ enabled the determination of as many as 32 energy levels in the 16 000−32 000 cm^{-1} spectral range. A preliminary simulation of the energy levels and transition intensities using Hamiltonian parameters for the f−d interactions reported in ref 17 shows that the number of experimental data is almost equal to the number of transitions with observable intensities (assuming that the peak is observable if its intensity is not smaller than 1% of the highest intensity peak). Therefore, given a relatively large experimental data set, one may try to determine the parameter values by fitting them to the experimental levels.

For calculation of the f−d spectra by using the Hamiltonian of eq 2, the crystal-field interaction parameters for the 5f electrons are needed. Hitherto, such parameters for the U^{3+} ion in cubic coordination have not been reported in the scientific literature. These parameters could not have been determined from the experimental spectrum because for $SrCl_2-U^{3+}(O_h)$ crystals codoped with NaCl, the oscillator strengths of the electric-dipole forbidden f−f transitions were too weak for unequivocal assignment of the energy levels. The elpasolite-type Cs_2NaYCl_6 crystals, in which U^{3+} ions substitute for Y^{3+} in the site of octahedral symmetry, may be viewed as the host most closely related to $SrCl_2$, for which the crystal-field parameters of U^{3+} are known. In both octahedral and cubic coordination, there are only two independent crystal-field parameters, B^4_0 and B^6_0, because parameters B^4_4 and B^6_4 are related to those with $q = 0$ by the $B^4_4/B^4_0 = (5/14)^{1/2}$ and $B^6_4/B^6_0 = (-7/2)^{1/2}$ ratios. Moreover, the B^k_q parameters for the cube can be linked to those for the octahedron: B^4_q(cube) = $-8/9B^4_q$(octahedron) and B^6_q(cube) = $64/27B^6_q$(octahedron). However, not only the coordination geometries but also the central-ion−ligand distances are different for Cs_2NaYCl_6 (2.619 Å) and $SrCl_2$ (3.021 Å) hosts. In a point-charge electrostatic model, parameters B^4_q and B^6_q depend on the distance R as $1/R^5$ and $1/R^7$, respectively. For the B^4_0 and B^6_0 parameters of U^{3+} in Cs_2NaYCl_6, the values of 4647 and 278 cm^{-1} were reported, respectively.[23] However, the results of ab initio theoretical studies[24] suggest that there is some misorder concerning the proposed assignment of irreducible representations to experimental energy levels in ref 23. This suggestion is further supported by our recent energy level analysis for $U^{3+}-Cs_3Lu_2Cl_9$ crystals,[25] which are closely related structurally to Cs_2NaYCl_6. When the calculations were repeated for $U^{3+}-Cs_2NaYCl_6$ with the corrected energy-level assignment, they resulted in slightly different values than those of the B^k_q parameters reported previously, equal to 4140 and 565 cm^{-1} for B^4_0 and B^6_0, respectively, which are now similar to those determined for Cm^{3+} in Cs_2NaYCl_6 ($B^4_0 = 4034$ and $B^6_0 = 664$ cm^{-1}).[26] The relations given above between the parameters in cubic and octahedral coordinations allow one to estimate values of −1800 and 490 cm^{-1} for the B^4_0 and B^6_0 parameters of U^{3+} in $SrCl_2$, respectively. The values obtained are similar to those determined for Nd^{3+} in CaF_2 ($B^4_0 = -1900$ and $B^6_0 = 500$ cm^{-1}).[27] It is not unexpected because although the crystal-field strength is about a factor of 2 larger for the 5f ion than it is for the 4f ion, this effect is compensated to a great extent by a weaker crystal field exerted by chloride ligands compared to that of fluoride ligands. Consequently, for crystal-field interactions of 6d electrons, we used the values determined for Ce^{3+} in CaF_2.[15] In contrast to the B^k_q parameters, which are very sensitive to the structure of the energy levels, the $F^k(ff)$, $\zeta(ff)$, and the other free-ion parameters are not expected to change significantly for the same ion in different crystals, and therefore the values determined for the U^{3+} ion in $LaCl_3$ were taken as the starting values of the parameters for atomic *ff* interactions.[28] The parameters for Coulomb interactions between the $5f^2$ electrons and the $6d^1$ electron have been obtained from free-ion ab initio calculations using standard atomic computer programs.[29] The initial values of the Hamiltonian parameters are included in column 2 of Table 2.

In the first step of the analysis, taking into account the barricenters and the relative intensities of the three most intense bands (A1, A2, and A3 in Figure 1), the amount of reduction of the $F^k(fd)$and $G^j(fd)$ parameters from the ab initio calculated free-ion values was roughly evaluated. Then, the experimental energy levels were assigned to the nearest calculated values, providing that the appropriate transition had a calculated intensity large enough to be observable. Whenever two or more assignments were possible, the calculated level with the larger predicted intensity was chosen. For the calculation of the energy levels and transition intensities, we used the extended f-shell empirical programs written by M. Reid.[30] The parameters of the Hamiltonian were optimized by minimizing the squares of the differences between the experimental and calculated energy levels. In the final step, 10 parameters were varied and determined simultaneously. The final parameter values are shown in column 3 of Table 2. The transitions from $5f^3$ to the $5f^26d^1$ configuration are electric-dipole allowed, and the appropriate matrix elements for the transitions can be calculated using the expressions described in ref 17. Nevertheless, because of the difference between the equilibrium distances of the metal ion and the ligand in the ground and excited states, resulting from the larger extent of 6d orbitals compared to the 5f orbitals, most of the transition intensity is in the vibronic bands.[20] However, the simulation of the vibronic transition intensities is beyond the scope of this paper. Moreover, because the per-

TABLE 2: Energy Parameters (All Values in cm^{-1} Except n) for the $5f^26d^1$ Configuration of U^{3+} in $SrCl_2$[h]

parameter	value: initial	value: final
$F^2(ff)$	38269[28]	42855(1200)
$F^4(ff)$	30530[28]	32917(1990)
$F^6(ff)$	19770[28]	23570[a]
$\alpha(ff)$	[31,0][28]	[31,0][28]
$\beta(ff)$	[−886][28]	[−886][28]
$\gamma(ff)$	[2059][28]	[2059][28]
$\zeta_{5f}(ff)$	1612[28]	1804(16)
$M^0(ff)$[b]	[0.67][28]	[0.67][28]
$P^2(ff)$[b]	[1579][28]	[1579][28]
$B^4_0(ff)$[c]	−1800	−1620(400)
$B^6_0(ff)$[c]	490	1456(220)
$\Delta_E(fd)$		24912(120)
$F^2(fd)$	34549[29]	13347(620)
$F^4(fd)$	19036[29]	11010(1730)
$G^1(fd)$	20273[29]	9201(270)
$G^3(fd)$	15532[29]	7422(1410)
$G^5(fd)$	11817[29]	5363[d]
$\zeta(dd)$	2714[29]	2714[29]
$B^4_0(dd)$[e]	−44016[15]	−44016[15]
n[f]		32
rms[g]		95

[a] The $F^6(ff)$ parameter was constrained by the fixed ratio: $F^6(ff)/F^2(ff) = 0.55$. [b] The $M^2(ff)$, $M^4(ff)$, $P^4(ff)$ and $P^6(ff)$ parameters were constrained by the Hartree−Fock determined fixed ratios: $M^2(ff) = 0.55M^0(ff)$, $M^4(ff) = 0.38M^0(ff)$, $P^4(ff) = 0.5P^2(ff)$ and $P^6(ff) = 0.1P^2(ff)$. [c] $B^4_4(ff) = \sqrt{(5/14)}B^4_0 = -908\ cm^{-1}$, $B^6_4(ff) = -\sqrt{(7/2)}B^6_0 = -2511\ cm^{-1}$. [d] The $G^5(fd)$ parameter was constrained by the free-ion fixed ratio: $G^5(fd)/G^1(fd) = 0.583$, calculated using Cowan's code. [e] $B^4_4(ff) = \sqrt{(5/14)}B^4_0 = -28686\ cm^{-1}$. [f] Number of experimental energy levels included in the fitting procedure. [g] Deviation rms $= \sum_i[(\Delta_i)^2/(n-p)]^{1/2}$, where Δ_i is the difference between the observed and calculated energies, n is a number of levels fitted, and p is the number of parameters freely varied. [h] The fitted values are followed by numbers in parentheses, which indicate the uncertainties of the determined parameter values. Parameters in square brackets were kept at constant values during the fitting procedure. Parameters for the splitting of the $5f^5$ core (other than the parameters for Coulomb and spin−orbit interactions) are obtained from the literature[28] (values for the $5f^5$ configuration of U^{3+} in $LaCl_3$). The spin−orbit interaction parameter of the 6d electron is calculated using Cowan's code[29] (free-ion value). For the crystal-field splitting of the 6d state, the parameters determined for Ce^{3+} in CaF_2 (ref 15) were applied.

formed calculations yield energies of electronic origins, we prefer to compare them with the positions of the experimental zero-phonon lines instead of attempting to simulate the whole spectrum profile. The calculated and experimental energy levels as well as the relative transition intensities are listed in Table 3. From the 68 crystal field energy levels predicted by the theory between 16 000 and 30 000 cm^{-1}, 32 levels were identified and included in the calculations. Because the transition to only one of the unassigned levels (at 21 573 cm^{-1}) has a predicted intensity larger than 2.5% of the most intense line, one is allowed to state that almost all of the transitions observable in the spectrum have been identified. The calculated energy levels are also shown graphically by the sticks at the bottom of Figures 2−4 and may be compared to the experimentally determined positions of zero-phonon lines, which are indicated by arrows.

The largest difference between the experimental (at 16 330 cm^{-1}) and calculated level is equal to −193 cm^{-1}, and the root-mean-square (rms) deviation defined as rms $= (\sum(E_{exptl} - E_{calcd})^2/(n-p))^{1/2}$ amounts to 95 cm^{-1} for $n = 32$ fitted levels and $p = 10$ varied parameters. As one could expect, because of the significantly stronger CF effect, the obtained rms value is larger than the values reported for the $5f^3$ configuration of U^{3+} in strong high-symmetry crystal fields, which usually amount to 50−60 cm^{-1} [31] but is comparable to rms deviations resulting from the analysis of the $5f^2$ configuration of U^{4+}.[32] Although

TABLE 3: Calculated and Experimental Energy Levels for the $5f^56d(e_g)^1$ Configuration of the U^{3+} Ion in $SrCl_2$ Single Crystals

level[a]	irrep.[b]	energy (cm^{-1}): E_{calcd}	E_{exptl}	$E_{exptl} - E_{calcd}$	relative transition intensity[c]
$37(^3H)^4K_{11/2}$, $15(^3H)^4I_{9/2}$	Γ_8	16 275	16 213	−63	19.30
$48(^3H)^4K_{11/2}$, $24(^3H)^4G_{5/2}$	Γ_7	16 523	16 330	−193	1.27
$35(^3H)^4K_{11/2}$, $13(^3H)^4I_{11/2}$	Γ_6	16 592	16 736	144	17.68
$51(^3H)^4K_{11/2}$, $14(^3H)^4F_{3/2}$	Γ_8	16 788	16 869	81	8.29
$52(^3H)^4I_{9/2}$, $12(^3H)^4H_{7/2}$	Γ_8	16 918	17 007	103	19.66
$24(^3H)^4I_{9/2}$, $21(^3H)^2H_{9/2}$	Γ_8	17 459	17 310	−149	66.36
$26(^3H)^2H_{9/2}$, $16(^3H)^4I_{9/2}$	Γ_6	17 701	17 606	−95	30.42
$24(^3H)^4H_{7/2}$, $11(^3H)^4I_{11/2}$	Γ_6	18 215			0.03
$20(^3H)^4H_{13/2}$, $10(^3H)^4F_{5/2}$	Γ_7	18 573	18 563	−10	3.95
$19(^3H)^4H_{7/2}$, $11(^3H)^2G_{7/2}$	Γ_8	18 606	18 599	−7	45.76
$21(^3H)^4K_{13/2}$, $14(^3H)^4F_{5/2}$	Γ_8	18 744	18 727	−17	0.77
$26(^3H)^4K_{13/2}$, $16(^3H)^4G_{7/2}$	Γ_7	18 820	18 918	98	1.12
$31(^3F)^4H_{7/2}$, $16(^3F)^4P_{1/2}$	Γ_6	20 854	20 942	87	24.86
$33(^3F)^4H_{7/2}$, $8(^3F)^4D_{3/2}$	Γ_8	20 983	20 991	8	100.00
$38(^3F)^4G_{5/2}$, $13(^3F)^4H_{7/2}$	Γ_7	21 141	21 101	−40	3.72
$9(^3F)^4F_{5/2}$, $12(^3H)^4K_{13/2}$	Γ_8	21 505	21 502	−3	7.30
$23(^3F)^4D_{1/2}$, $16(^3F)^4H_{9/2}$	Γ_6	21 573			2.91
$21(^3F)^4G_{7/2}$, $17(^3F)^4H_{7/2}$	Γ_7	21 815			1.71
$11(^3F)^4G_{7/2}$, $11(^3H)^4I_{11/2}$	Γ_8	22 144	22 178	34	2.45
$22(^3H)^4I_{11/2}$, $12(^3H)^4I_{13/2}$	Γ_6	22 638			0.04
$20(^3H)^4I_{13/2}$, $15(^3H)^2H_{11/2}$	Γ_7	22 667			0.23
$13(^3H)^4I_{11/2}$, $11(^3H)^4G_{9/2}$	Γ_8	22 726	22 671	−55	3.45
$21(^3H)^4H_{11/2}$, $17(^3H)^2H_{11/2}$	Γ_8	23 045	23 223	178	2.41
$15(^3H)^4K_{13/2}$, $14(^3H)^2I_{11/2}$	Γ_6	23 306			0.01
$15(^3H)^4K_{13/2}$, $14(^3H)^4G_{9/2}$	Γ_8	23 522	23 527	5	0.68
$28(^3H)^4K_{15/2}$, $24(^3H)^4F_{7/2}$	Γ_7	23 926			0.00
$12(^3H)^4H_{9/2}$, $11(^3H)^4K_{15/2}$	Γ_8	23 987			1.20
$29(^3H)^4K_{15/2}$, $21(^3H)^4F_{7/2}$	Γ_6	24 022	24 009	−13	1.53
$23(^3H)^4K_{15/2}$, $14(^3H)^4F_{7/2}$	Γ_8	24 161	24 123	−38	0.47
$20(^3H)^4K_{13/2}$, $12(^3H)^2K_{13/2}$	Γ_7	24 350			0.06
$24(^3H)^4H_{9/2}$, $17(^3H)^2H_{9/2}$	Γ_6	24 447			0.56
$13(^3H)^4H_{9/2}$, $13(^3H)^4K_{15/2}$	Γ_8	24 550	24 564	14	2.53
$16(^3F)^4H_{9/2}$, $13(^3F)^4G_{9/2}$	Γ_8	24 858	24 918	60	0.90
$9(^3F)^4H_{11/2}$, $9(^3F)^4G_{9/2}$	Γ_8	24 931			0.25
$12(^3H)^4K_{13/2}$, $11(^3H)^2K_{13/2}$	Γ_8	25 058			0.01
$21(^3H)^2G_{7/2}$, $20(^3H)^2K_{13/2}$	Γ_7	25 654			0.41
$26(^3F)^4H_{11/2}$, $16(^3F)^4P_{5/2}$	Γ_7	25 691			0.34
$17(^3F)^4G_{7/2}$, $14(^3F)^4F_{7/2}$	Γ_6	25 740			0.17
$19(^1G)^2G_{9/2}$, $16(^3F)^4F_{9/2}$	Γ_6	25 775			0.19
$12(^3F)^4G_{7/2}$, $12(^3F)^4F_{7/2}$	Γ_8	25 869	25 900	31	0.48
$16(^3F)^4H_{11/2}$, $11(^3F)^4D_{3/2}$	Γ_8	26 105	26 021	−84	1.22
$12(^3H)^2F_{5/2}$, $10(^3F)^4P_{5/2}$	Γ_8	26 303			0.31
$21(^3F)^4H_{11/2}$, $17(^3F)^4D_{7/2}$	Γ_6	26 383	26 392	9	2.75
$14(^3F)^4H_{13/2}$, $10(^3F)^4P_{5/2}$	Γ_7	26 584			0.00
$11(^3F)^4F_{5/2}$, $9(^3F)^4G_{9/2}$	Γ_8	26 621	26 560	−61	5.99
$12(^3F)^4F_{9/2}$, $11(^3F)^4D_{5/2}$	Γ_8	26 984	27 012	28	2.52
$13(^3F)^4D_{7/2}$, $12(^3F)^2G_{7/2}$	Γ_7	27 109			0.16
$19(^3F)^2P_{1/2}$, $19(^3F)^2H_{9/2}$	Γ_6	27 155	27 130	−25	0.81
$9(^3H)^2G_{7/2}$, $6(^3F)^2H_{11/2}$	Γ_7	27 317			0.03
$20(^3H)^4I_{15/2}$, $10(^3F)^2H_{11/2}$	Γ_8	27 400			0.13
$10(^3F)^2H_{9/2}$, $10(^3F)^2D_{3/2}$	Γ_8	27 546			0.41
$23(^3F)^2F_{7/2}$, $16(^1G)^2G_{7/2}$	Γ_6	27 601			0.02
$21(^3H)^4I_{15/2}$, $12(^1G)^2I_{11/2}$	Γ_8	27 612			0.03
$27(^3H)^4I_{15/2}$, $25(^3H)^4H_{13/2}$	Γ_7	27 779			0.10
$25(^3H)^4I_{15/2}$, $19(^3H)^4G_{11/2}$	Γ_8	27 881			0.11
$11(^1G)^2H_{9/2}$, $10(^3F)^2G_{9/2}$	Γ_8	28 004			0.08
$26(^3H)^4K_{17/2}$, $22(^3H)^4G_{11/2}$	Γ_6	28 294			0.06
$9(^3H)^4H_{11/2}$, $8(^3F)^2G_{7/2}$	Γ_7	28 385			0.00
$27(^3H)^4K_{17/2}$, $26(^3H)^4F_{9/2}$	Γ_8	28 509			0.36
$35(^3H)^4H_{13/2}$, $11(^3H)^4K_{17/2}$	Γ_8	28 663	28 590	−73	1.11
$33(^3H)^4H_{13/2}$, $14(^3H)^4K_{17/2}$	Γ_7	28 751			0.06
$37(^3H)^4K_{17/2}$, $24(^3H)^4F_{9/2}$	Γ_6	29 166			0.04
$15(^3H)^2H_{11/2}$, $13(^3H)^2I_{13/2}$	Γ_8	29 219	29 184	−35	0.26
$19(^1G)^2I_{11/2}$, $11(^1G)^2F_{5/2}$	Γ_7	29 243			0.07
$19(^3H)^4K_{17/2}$, $12(^3H)^4F_{9/2}$	Γ_8	29 345			0.16
$13(^3F)^2F_{5/2}$, $11(^1G)^2H_{9/2}$	Γ_8	29 624	29 615	−9	0.46
$35(^3H)^2I_{13/2}$, $13(^3H)^2G_{9/2}$	Γ_6	29 645			0.00

[a] Only the largest components (in percentage) of the $\{[(S_fL_f)SL_f]J;e_g\}$ eigenstates are indicated. [b] Irreducible representation. [b] Predicted values; the transition intensity is proportional to the line strength multiplied by the transition energy.

TABLE 4: Calculated Free-Ion Parameters (by Using Cowan's Atomic Programs[29]) for the $5f^3$, $5f^2$, and $5f^2 6d^1$ Configurations of Uranium Ions

parameter	value (cm^{-1})		
	$5f^3$	$5f^2$	$5f^2 6d^1$
$F^2(ff)$	71 556	76 802	75 206
$F^4(ff)$	46 449	50 253	49 086
$F^6(ff)$	33 971	36 894	35 996
$\zeta(ff)$	1906	2117	2064

the location of the $5f^2 6d(e_g)^1$ configuration above the ground state is controlled by three parameters, $\Delta_E(fd)$, $B^4_0(dd)$, and $\zeta(dd)$, the Coulomb f−d(e_g) interactions are responsible for most of the splitting of the $5f^2 6d(e_g)^1$ states, and only small changes in the values of the Coulomb f−d interaction parameters are needed to shift the energy levels on the order of ~100 cm^{-1}. Additional inaccuracy may result from uncertainties in the determination of other parameters (e.g., $F^k(ff)$, $B^4_0(ff)$, or $\zeta(ff)$). Therefore, taking into account the large number of Hamiltonian parameters that had to be approximated or constrained, the overall agreement between the calculated and experimental energy levels may be regarded as quite good.

Only the energy levels of the $5f^2 6d(e_g)^1$ configuration were included in the calculations. As a consequence of this, the $B^k_q(dd)$ and $\zeta(dd)$ parameters, which depend on the position and splitting of the $5f^2 6d(t_{2g})^1$ states, could not be fitted. Therefore, the spin−orbit parameter was fixed at the free-ion value obtained from the ab initio calculations, whereas the 6d electron crystal-field interaction parameters were kept at constant values, the same as those for Ce^{3+} in CaF_2 ($B^4_0(dd) = -44\,016$ and $B^6_0 = -26\,305$ cm^{-1}).[15]

In the final fit, we have adjusted values of $\Delta_E(fd)$, $F^k(ff)$ ($k = 2, 4$), $\zeta(ff)$, $B^k_0(ff)$ ($k = 4, 6$), $F^k(fd)$ ($k = 2, 4$), and $G^j(fd)$ ($k = 1, 3$) parameters. The $F^2(ff)$ and $F^4(ff)$ Slater integrals increased their values by 12.0 and 7.8%, respectively, and the $\zeta(ff)$ spin−orbit parameter increased by 11.9% compared to the presumed values of the $5f^3$ configuration. Because the attempts to release of the $F^6(ff)$ parameter have led to an unphysical solution, this parameter was fixed at a constant ratio relative to $F^2(ff)$: $F^6(ff)/F^2(ff) = 0.55$. The larger values of the $F^k(ff)$ parameters for the $5f^2 6d$ configuration when compared to those for the $5f^3$ configuration are in line with the expectations and result from contraction of the 5f orbitals in the $5f^2 6d$ configuration. In simulations of lanthanide spectra, these parameters were increased by 6% (based on the ratio between the ab initio calculated free-ion values for the $4f^{n-1}5d$ and $4f^n$ configurations) from values obtained from analysis of $4f^N$ energy levels.[15,16] In our calculations for the actinide ion, this increase is significantly larger. However, the results of Hartee−Fock calculations shown in Table 4 suggest that although the free-ion values of the $F^k(ff)$ and $\zeta(ff)$ parameters for the $5f^2 6d^1$ configuration are placed between the values for the $5f^3$ and $5f^2$ configurations, they are closer to the latter ones. The results obtained in our calculations are in fair agreement with this prediction because the determined values of the $F^k(ff)$ and $\zeta(ff)$ parameters are similar to those typical for the $5f^2$ configuration of U^{4+} in a chloride environment.[33,34] This allows us to state that the determined values of the $F^k(ff)$ and $\zeta(ff)$ parameters for the $5f^2 6d^1$ configuration are reasonable.

The next parameters that were adjusted in the fitting procedure were parameters for direct and exchange Coulomb f−d interactions. The parameters $F^2(fd)$ and $F^4(fd)$ could be fitted independently, and the resulted values are reduced to 38.6 and 57.8% of the initial Hartree−Fock free-ion values, respectively. This reduction is considerably larger than that for lanthanide ions, in which the $F^k(fd)$ parameters were typically reduced to about 67% of their ab initio calculated free-ion values.[15,16] The larger reduction for the actinide ion compared to lanthanide ions may be linked to the larger extension of 5f and 6d orbitals with respect to the 4f and 5d orbitals, which leads to adequately larger delocalization of 5f and 6d electrons over the ligands in crystalline hosts. However, the decrease in the $F^k(fd)$ parameters is smaller than that obtained for U^{3+} in $LiYF_4$, in which a reduction to 33% of the ab initio calculated free-ion values was assumed.[17] However, this relation is in contradiction with the expected trend because a larger reduction is expected for the more covalent ligands, and Cl^- is more covalent than F^-. It seems that some other analyses for the U^{3+} ion in different hosts would be required for an explanation of this discrepancy.

In hitherto performed analyses, the fixed ab initio calculated ratio between $F^2(fd)$ and $F^4(fd)$ parameters has been retained, even though the free-ion data for lanthanide ions indicate that ab initio calculations overestimate mainly the value for the $F^2(fd)$ parameter.[35] The free-ion data are not available for uranium ions, however, a similar trend should be expected. The results of our fit are in accordance with this assumption because the $F^2(fd)$ parameter is considerably more reduced than $F^4(fd)$. Moreover, the trend observed for the $F^k(fd)$ parameters stays in agreement with the relative reduction of the $F^2(ff)$ and $F^4(ff)$ parameters with respect to their ab initio calculated free-ion values.

Both the $G^1(fd)$ and $G^3(fd)$ parameters are reduced by similar amounts to 45.4 and 47.8% of their ab initio calculated free-ion values, respectively. Although the difference is small, the observed trend is in line with the expectations that the ab initio calculations overestimate the value of the $G^1(fd)$ parameter by a larger amount than those of the $G^3(fd)$ or $G^5(fd)$ parameters. The $G^5(fd)$ parameter could not have been adjusted independently because such attempts led to an unrealistic value, so it was constrained by the $G^5(fd)/G^1(fd)$ Hartree−Fock free-ion ratio. Some problems with the determination of the $G^5(fd)$ parameter value may result from the fact that the $G^j(fd)$ parameters depend mostly on the energy differences between the first spin-forbidden and spin-allowed f−d transitions, which obviously could not have been determined for the U^{3+} ion.

It has been shown in ref 1 that a simple model assuming the coupling of crystal-field levels of the $6d^1$ electron with the lattice and the multiplet structure of the $5f^{N-1}$ configuration are able to account for the general feature of the spectra of U^{3+} in UCl_6^{3-} complexes and enables assignment of the main characters of the excited states of the $5f^{N-1}6d^1$ manifold, which are giving rise to a particular group of energy levels. Because the effects of Coulomb interactions between 5f and 6d electrons were neglected in this qualitative model, the interesting question arises: how important is the influence of these effects on the energy-level structure? In Figure 5a, the splitting of $5f^2 6d^1$ levels in the 16 000−32 000 cm^{-1} energy region is presented as a function of the magnitude of the $F^k(fd)$, $G^j(fd)$, and $\zeta(dd)$ parameters. The A parameter used as a horizontal axis multiplies the values of the $F^k(fd)$, $G^j(fd)$, and $\zeta(dd)$ parameters. For $A = 0$, which corresponds to omitting the interactions connected with the $F^k(fd)$, $G^j(fd)$, and $\zeta(dd)$ parameters in the Hamiltonian defined in eq 2, the energy-level structure matches the multiplet structure of the $5f^2(U^{4+})$ configuration, which is shown schematically on the extreme left-hand side of Figure 5a. The increase of A is accompanied by an increase in the spitting of the states, and for $A = 1$, a dense array of energy levels is observed. However, even for $A = 1$, which corresponds to the

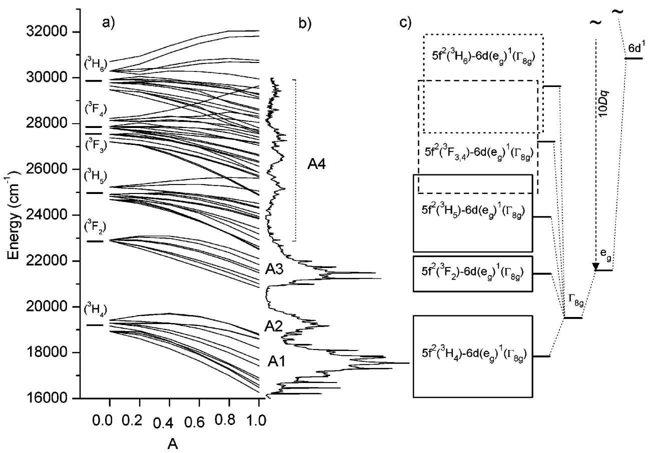

Figure 5. (a) Splitting of the $5f^26d^1$ crystal-field components observed in the 16 000−32 000 cm^{-1} energy range. Coefficient *A* multiplies the $F^k(fd)$, $G^j(fd)$ and $\zeta(dd)$ parameters of the Hamiltonian defined in eq 2 associated with f−d Coulomb and 6d spin−orbit interactions. For $A = 1$, those parameters assume values equal to those quoted in column 3 of Table 3. On the left-hand side, the multiplet structure of the $5f^2$ configuration is shown schematically. (b) Experimental 4.2 K absorption spectrum of U^{3+}−$SrCl_2$. (c) Schematic diagram showing the energy levels for U^{3+} in cubic O_h coordination. Only the lowest-energy $5f^2$-$(^{2S+1}L_J)$−$6d(e_g)^1(\Gamma_{8g})$ levels arising from the coupling of $5f^2$ core electrons ($^3H_4$, $^2F_2$, and $^3H_5$ substates) and 6d electrons ($5f^26d(e_g)^1$ configuration) are included.

values of the $F^k(fd)$, $G^j(fd)$, and $\zeta(dd)$ parameters, such as those presented in column 3 of Table 2 for the $5f^26d^1$ configuration of U^{3+}, the groups of levels which may be related to the $^3H_4$ and $^3F_2$ substates of the $5f^2$ core are not mixed. Similarly, levels associated with the $^3H_5$ multiplet of the $5f^2$ core are also well separated because only the two highest energy crystal-field levels originating from this state overlap with the two lowest components of the ($^3F_3$ + $^3F_4$) multiplets. This justifies the application of qualitative reasoning, assuming a superposition of the multiplet structure of the $5f^2$ core on the $6d^1$ crystal-field levels, for rationalization of the U^{3+} f−d spectrum in the 16 000−26 000 cm^{-1} energy region, where the most intense f−d transitions of U^{3+}−$SrCl_2$ are observed (Figure 5b). A simplified diagram showing the energy-level structure of U^{3+} in $SrCl_2$ in the 16 000−26 000 cm^{-1} energy range is presented in Figure 5c. The U^{3+} ion in the $SrCl_2$ crystal has a cubic 8-fold coordination, and the crystal field splits the $6d^1$ electronic state into an e_g lower and a t_{2g} upper state (not shown in the diagram). The e_g level of Γ_{8g} symmetry is not split by a spin−orbit interaction. The three lowest energy groups of the levels result from the interaction of the $6d(e_g)\Gamma_{8g}$ state with the $5f^2(^3H_4)$, $5f^2(^3F_2)$, and $5f^2(^3H_5)$ core electron substates and can be described as $5f^2(^3H_4)$−$6d(e_g)^1(\Gamma_{8g})$, $5f^2(^3F_2)$−$6d(e_g)^1(\Gamma_{8g})$, and $5f^2(^3H_5)$−$6d(e_g)^1(\Gamma_{8g})$, respectively. Therefore, the bands marked in Figure 5b as A1 and A2, starting at 16 200 cm^{-1} and extending to ∼19 800 cm^{-1}, are formed by transitions to the crystal-field levels arising from the $5f^2(^3H_4)$−$6d(e_g)^1(\Gamma_{8g})$ configuration, whereas band A3 centered at ∼21 500 cm^{-1} should be attributed to transitions to levels originating from the $5f^2(^3F_2)$−$6d(e_g)^1(\Gamma_{8g})$ configuration. The lower intensity bands observed between 23 000 and 30 000 cm^{-1} (group A4) are due to transitions to levels resulting from the interaction of the $6d(e_g)\Gamma_{8g}$ state with the excited $5f^2(^3H_{5,6})$ and $5f^2(^3F_{3,4})$ substates. Because the Coulomb interaction between *nf* and $(n + 1)$d electrons is responsible for most of the splitting of the $nf(n + 1)$d states (Figure 5a), and this interaction between the 4f and 5d electrons is larger than that between the 5f and 6d electrons, it may be expected that such a simplified model will be less valid for lanthanide ions. Moreover, it should be noticed that the energy-level structure will be more complex for *nf*-electron ions in an octahedral (O_h) 6-fold coordination, in which the order of the t_{2g} and e_g crystal-field states is reversed, and the lower t_{2g} state is split additionally by the spin−orbit interaction into a Γ_{8g} degenerate quartet and a higher-lying Γ_{7g} Kramer's doublet.

5. Summary

In this paper, a low-temperature $5f^3 \rightarrow 5f^26d^1$ absorption spectrum of U^{3+} in $SrCl_2$ single crystals has been presented. The only phonon line that was observed in the spectrum corresponds to a ∼247 cm^{-1} $\nu_1(a_{1g})$ stretching mode, which, in connection with relatively weak electron−lattice coupling (Huang−Rhys parameter value of $S(a_{1g}) \approx 1.5$ was determined), makes the absorption-line assignment relatively straightforward. Between 16 000 and 32 000 cm^{-1}, as many as 32 zero-phonon lines corresponding to transitions from the ground $^4I_{9/2}$ state of the $5f^3$ configuration to crystal-field levels of the excited $5f^2$-$6d(e_g)^1$ configuration were identified. The transitions to $5f^26d$-$(t_{2g})^1$ states expected at an energy >38 000 cm^{-1} are weak, and none of the zero-phonon lines could be assigned unambiguously.

For the analysis of the energy levels, the extended model developed by Reid et. al.[14] has been applied. The Hamiltonian parameters for the Coulomb interaction between 5f electrons ($F^k(ff)$, $k = 2, 4$), the spin−orbit interaction of the 5f electron ($\zeta_{5f}(ff)$), the crystal-field interactions of the $5f^2$ electrons with the lattice ($B_0^4(ff)$ and $B_0^6(ff)$), and the Coulomb interactions between the 6d electron and the $5f^2$ electrons ($F^k(fd)$, $k = 2, 4$ and $G^j(fd)$, $j = 1, 3$) were determined by least-squares fitting of the calculated energies to the experimental data. The overall agreement between the calculated and experimentally observed energy levels is quite good, with the root-mean-square (rms) deviation equal to 95 cm^{-1} for 32 fitted levels and 10 varied parameters. Adjusted values of the $F^k(ff)$ and $\zeta_{5f}(ff)$ parameters for the $5f^2$ core electrons are closer to the values of the $5f^2$-(U^{4+}) configuration than to those of the $5f^3(U^{3+})$ configuration, which stays in line with the atomic parameters predicted by Cowan's computer code. The $F^2(fd)$ and $F^4(fd)$ parameters are reduced to 38.6 and 57.8% of the initial free-ion Hartree−Fock values, respectively, and a similar decrease to ∼46% of the ab initio calculated free-ion values was observed for the $G^j(fd)$ exchange Slater parameters. The amount of reduction is considerably larger than that for lanthanide ions, for which the parameters were reduced typically to about 67% of their calculated free-ion values[35] but smaller than that for U^{3+}−$LiYF_4$, for which the f−d interaction parameters were decreased to ∼33% of the calculated free-ion values.[17] The larger reduction of $F^2(fd)$ parameter compared to that of $F^4(fd)$ is in accordance with the free-ion data for lanthanide ions, which show that ab initio calculations overestimate mainly the values for the F^2-(fd) parameter and is also in agreement with the trend apparent for the $F^2(ff)$ and $F^4(ff)$ parameters.

One should be aware that the calculated energies are affected by a large number of Hamiltonian parameters, and their adjusted values depend strongly on the experimental energy-level assignment, which in some cases was not unambiguous. Therefore, although the obtained set of parameters describes the experimental spectrum well, some other calculations for U^{3+} ions in other hosts would be required to prove the correctness of the obtained values and to track trends in the parameters.

Because of the larger extent of 5f and 6d orbitals compared to 4f and 5d orbitals, the f−d interactions are smaller for U^{3+} than for the isoelectronic Nd^{3+} lanthanide ion. As a result of this, the groups of bands in the 16 000−32 000 cm^{-1} region may be related directly to the multiplet structure of the $5f^2$-(U^{4+}) configuration. This justifies employing for the qualitative analysis of the f−d spectrum of the U^{3+} ion, the very simple model assuming the coupling of crystal-field levels of the $6d^1$ electron with the lattice and the multiplet structure of the $5f^2$ configuration. It accounts for general structure of the spectra and allows us to assign the main characters of the excited states of the $5f^26d^1$ manifold, which are giving rise to a particular group of energy levels.

Acknowledgment. I thank Professor M. F. Reid (University of Canterbury, New Zealand) for providing the extended f-shell empirical programs.

References and Notes

(1) Karbowiak, M.; Drożdżyński, J. *J. Phys. Chem. A* **2004**, *108*, 6397.
(2) Dorenbos, P. *J. Lumin.* **2000**, *91*, 155.
(3) Kaminskaya, A. N.; Drożdżyński, J.; Mikheev, N. B. *Radiokhimiya* **1980**, *22*, 247.
(4) Kaminskaya, A. N.; Drożdżyński, J.; Mikheev, N. B. *Radiokhimiya* **1981**, *23*, 264.
(5) Mazurak, Z.; Drożdżyński, J.; Hanuza, J. *J. Mol. Struct.* **1988**, *171*, 443.
(6) Drożdżyński, J. *Acta Phys. Pol., A* **1993**, *84*, 975.
(7) Seijo, L.; Barandiaran, Z. *J. Chem. Phys.* **2003**, *118*, 5335.
(8) Sytsma, J.; Piehler, D.; Edelstein, N. M.; Boatner, L. A.; Abraham, M. M. *Phys. Rev. B* **1993**, *47*, 14786.
(9) Marsman, M.; Andriessen, J.; van Eijk, C. W. E. *Phys. Rev. B* **2000**, *61*, 16477.
(10) Chase, L. L. *Phys. Rev. B* **1970**, *2*, 2308.
(11) Weakliem, H. A. *Phys. Rev. B* **1972**, *6*, 2743.
(12) Johnson, K. E.; Sandoe, J. N. *J. Chem. Soc. A* **1969**, 1694.
(13) Meijerink, A.; Wegh, R. T.; van Pieterson, L. *Proc. Electrochem. Soc.* **2000**, *99−40*, 23.
(14) Reid, M. F.; van Pieterson, L.; Wegh, R. T.; Meijerink, A. *Phys. Rev. B* **2000**, *62*, 14744.
(15) van Pieterson, L.; Reid, M. F.; Wegh, R. T.; Soverna, S.; Meijerink, A. *Phys. Rev. B* **2002**, *65*, 045113.
(16) van Pieterson, L.; Reid, M. F.; Burdick, G. W.; Meijerink, A. *Phys. Rev. B* **2002**, *65*, 045114.
(17) Ning, L.; Jiang, Y.; Xia, S.; Tanner, P. A. *J. Phys.: Condens. Matter* **2003**, *15*, 7337.
(18) Drożdżyński, J. *J. Less-Common Met.* **1988**, *138*, 271.
(19) Pack, D. W.; Manthey, W. J.; McClure, D. S. *Phys. Rev. B* **1989**, *40*, 9930.
(20) Henderson, B.; Imbusch, G. F. *Optical Spectroscopy of Inorganic Solids;* Clarendon Press: Oxford, U.K., 1989.
(21) Reber, C.; Güdel, H. U.; Meyer, G.; Schleid, T.; Daul, C. A. *Inorg. Chem.* **1989**, *28*, 3249.
(22) Tanner, P. A.; Mak, C. S. K.; Edelstein, N. M.; Murdoch, K. M.; Liu, G.; Huang, J.; Seijo, L.; Barandiarán, Z. *J. Am. Chem. Soc.* **2003**, *125*, 13225.
(23) Karbowiak, M.; Drożdżyński, J.; Hubert, S.; Simoni, E.; Stręk, W. *J. Chem. Phys.* **1998**, *108*, 10181.
(24) Seijo, L. Unpublished results.
(25) Karbowiak, M.; Mech, A.; Drożdżyński, J.; Ryba-Romanowski, W.; Reid, M. F. *J. Phys. Chem. B* **2005**, *109*, 155.
(26) Murdoch, K. M.; Cavalec, R.; Simoni, E.; Karbowiak, M.; Hubert, S.; Illemassene, M.; Edelstein, N. M. *J. Chem. Phys.* **1998**, *108*, 6353.
(27) Lesniak, K. *J. Phys.: Condens. Matter* **1990**, *2*, 5563.
(28) Karbowiak, M.; Drożdżyński, J.; Sobczyk, M. *J. Chem. Phys.* **2002**, *117*, 2800.
(29) Cowan, R. D. *The Theory of Atomic Structure and Spectra;* University of California Press: Berkeley, CA, 1981.
(30) Reid, M. F. University of Canterbury, New Zealand. Private communication.
(31) Karbowiak, M.; Zych, E.; Dereń, P.; Drożdżyński, J. *Chem. Phys.* **2003**, *287*, 365.
(32) Karbowiak, M.; Mech, A.; Drożdżyński, J. *Chem. Phys.* **2005**, *308*, 135.
(33) Krupa, J. C. *Inorg. Chim. Acta* **1987**, *139*, 223.
(34) Karbowiak, M.; Mech, A.; Drożdżyński, J. *Phys. Rev. B* **2003**, *67*, 195108.
(35) Reid, M. F.; van Pieterson, L.; Meijerink, A. *J. Alloys Compd.* **2002**, *344*, 240.